Hierarchical level-clustering in two-dimensional harmonic oscillators

C. B. Whan
Department of Electrical Engineering and Computer Science, Massachusetts Institute of Technology, Cambridge, Massachusetts 02139
(Received 19 November 1996)

We present numerical results for the statistical distribution of energy level spacings in two-dimensional harmonic oscillators with the irrational frequency ratio $R \equiv \omega_1/\omega_2$. Unlike scaled level spacings, the distribution of the true energy level spacings is well behaved, and directly reflects the corresponding classical quasiperiodic motion. The histogram of the energy level spacings shows sharp peaks at discontinuous values which form a hierarchical rational approximations to R. The peak heights follow a characteristic inverse-square-law increase as the level spacing $\Delta\mathcal{E}$ decreases, indicating a form of level clustering rather than level repulsion as previously believed. We believe the failure of convergence in the scaled level spacing distribution is due to the lack of proper energy scales in the system, since the average (true) level spacing vanishes in the semiclassical limit. [S1063-651X(97)50904-4]

PACS number(s): 05.45.+b, 03.65.Sq

In the last two decades much progress has been made in understanding the correspondence between classical and quantum dynamics of Hamiltonian systems [1–3]. One manifestation of this correspondence is the different universality classes that the quantum mechanical level spacing distributions belong to, depending on whether the corresponding classical Hamiltonian system is integrable or chaotic [4,5]. For integrable systems, it was shown by Berry and Tabor [4], almost 20 years ago, that the generic level spacing distribution follows the Poisson's law of exponential decay with a maximum at zero (level clustering). The same authors also note that the harmonic oscillator (in higher than one dimension), possibly the simplest integrable system, does not follow this generic rule. Furthermore their numerical experiment indicated that for two-dimensional harmonic oscillators (2DHO's) with an incommensurate frequency ratio, there was some sort of level repulsion, common for systems with chaotic classical motion. Subsequent studies by Pandey and co-workers [6,7] improved the numerics of Ref. [4], and found that the scaled level spacing distribution $P(s)$ does not converge in the semiclassical limit. In contrast, Bleher [8] studied the true level spacing distribution from a mathematical point of view, and was able to derive some analytical results, emphasizing the discreteness and rigidity of the spectrum. More recently, there was an attempt [9] to introduce special averaging techniques in order to obtain a stable distribution, again a mathematical trick.

In this paper, we use numerical experiment as our tool, to study the 2DHO level spacing distribution from a more physical standpoint. This approach enables us to understand the relation between the quantum level spacing distribution and the corresponding classical trajectories. We also offer a physically appealing explanation of the difference between the distribution of the true level spacings and that of the scaled spacings. We demonstrate numerically that if one considers the real energy level spacing $\Delta\mathcal{E}$, instead of the scaled spacing s (we will discuss the explicit definition of s at the end of the paper), the level spacing distribution $P(\Delta\mathcal{E})$ is in fact well behaved and physically meaningful, even though the rigorous mathematical aspect of it is more subtle, as pointed out in Ref. [8]. We found that $P(\Delta\mathcal{E})$ is sharply peaked at a series of discontinuous values, with the peak heights following a characteristic inverse-square-law-like rise as $\Delta\mathcal{E}\to 0$, in agreement with Ref. [8]. It is interesting to note the similarity between the 2DHO and other quasiperiodic systems, where inverse-power-law-type level spectrum was also observed [10–12].

In terms of action-angle variables [2,3], a 2DHO is described by the following Hamiltonian:

$$\mathcal{H}(\mathbf{I}) = \mathbf{I}\cdot\boldsymbol{\omega} = I_1\omega_1 + I_2\omega_2, \tag{1}$$

where I_i $(i=1,2)$ are the two independent action variables, and ω_i are the two frequencies. The classical motion of this system is described by a pure rotation on a two-dimensional (2D) torus in the originally four-dimensional phase space. If the two frequencies are commensurate, i.e., $R \equiv \omega_1/\omega_2 = p/q$, is a rational number, then the motion is periodic since the trajectory on the torus will close on itself after p and q rotations in the two independent angular variables, respectively. If, however, the two frequencies are incommensurate (R is an irrational number), the system executes a quasiperiodic motion, and its trajectory never closes and will eventually cover the 2D torus uniformly.

Quantum mechanically, 2DHO also constitutes a simple textbook example, and its eigenfunctions and eigenvalues can be readily obtained by solving Schrödinger's equation. In this paper, however, we will follow the authors of Ref. [4] and use the Einstein-Brillouin-Keller (EBK) semiclassical quantization rule, which, in the case of harmonic oscillators, gives the same energy spectrum as the exact quantum mechanical calculation. According to the EBK rule, the energy levels are given by [3]

$$E_{\mathbf{m}} = \mathcal{H}[\mathbf{I} = (\mathbf{m} + \boldsymbol{\alpha}/4)\hbar] = \hbar\boldsymbol{\omega}\cdot\left(\mathbf{m} + \frac{\boldsymbol{\alpha}}{4}\right), \tag{2}$$

where $\mathbf{m} = (m_1, m_2)$ are non-negative integers and the Maslov index $\boldsymbol{\alpha} = (2,2)$ in this case. From now on we will drop the Maslov index (corresponding to the zero-point energy) in the above expression since it does not affect the level statistics. Normalizing $E_{\mathbf{m}}$ in terms of $\hbar\omega_1$, we have

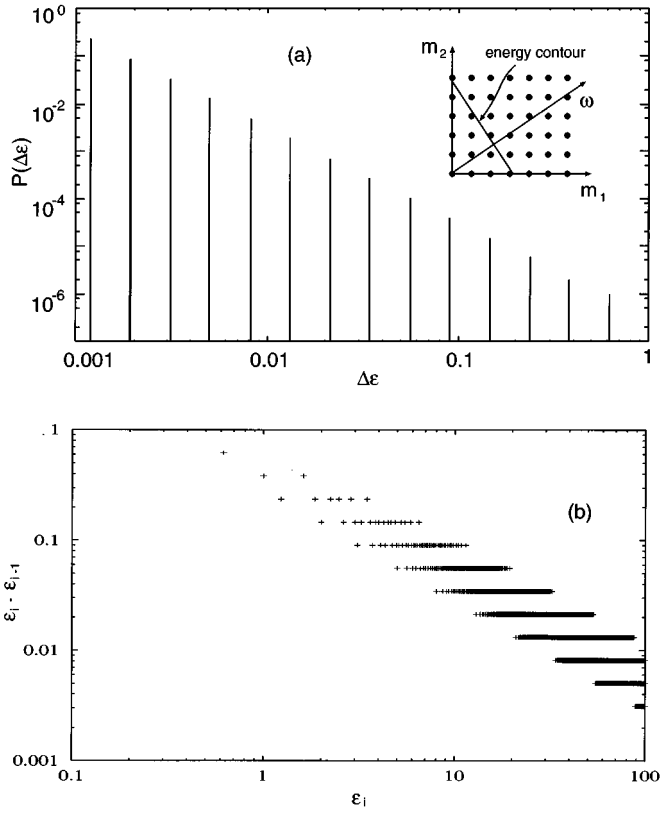

FIG. 1. (a) A histogram of the nearest neighbor level spacings for a two-dimensional harmonic oscillator with frequency ratio given by the golden mean $R=\sigma_1=(\sqrt{5}-1)/2$. The plot is based on $N=10^6$ levels, and the number of bins is 10^5. Inset: a geometrical interpretation of the Einstein-Brillouin-Keller semiclassical quantization rule. (b) The level spacings plotted against the energy levels, illustrating the clustering of $\Delta\mathcal{E}$ on discrete values. Note that, starting from the third row, every row of horizontal points begins with energies, $\mathcal{E}\approx F_n$ $(n=1,2,\ldots)$, where F_n are the Fibonacci numbers.

$$\mathcal{E}_{\mathbf{m}}\equiv\frac{E_{\mathbf{m}}}{\hbar\omega_1}=m_1+m_2R. \tag{3}$$

The energy spectrum described by Eqs. (2) and (3) has a simple geometrical interpretation, illustrated in the inset of Fig. 1(a). If we think of a two-dimensional lattice with a unit lattice constant, then every lattice point $\mathbf{m}=(m_1,m_2)$ that lies in the positive quadrant of this lattice space corresponds to a possible energy level $\mathcal{E}_{\mathbf{m}}$. The value of $\mathcal{E}_{\mathbf{m}}$, according to Eq. (2), is obtained by projecting $\mathbf{m}$ onto the direction of the ''frequency vector'' $\boldsymbol{\omega}=(\omega_1,\omega_2)$. Since $\boldsymbol{\omega}$ is normal to the energy contour defined by $\mathbf{m}\cdot\boldsymbol{\omega}=\mathcal{E}$ (a line in this case), the entire spectrum can be obtained by sliding the energy contour up (increasing $\mathcal{E}$) starting at the origin and projecting any lattice point it crosses on the way onto $\boldsymbol{\omega}$.

Numerically we use Eq. (3) to generate *all* the energy levels up to a given maximum $\mathcal{E}_{\max}$ and sort them in ascending order. After this reordering, the energy levels can be labeled with a single index, i.e., $\mathcal{E}_{\mathbf{m}}\rightarrow\mathcal{E}_i$, where $i=0,1,2,\ldots,N(\mathcal{E}_{\max})$, and $\mathcal{E}_i\leqslant\mathcal{E}_{i+1}$. Here $N(\mathcal{E}_{\max})$ is the total number of levels with energy $\mathcal{E}\leqslant\mathcal{E}_{\max}$ [i.e., the total number of lattice points in the triangular region bounded by the coordinate axes and the energy contour, $\mathbf{m}\cdot\boldsymbol{\omega}=\mathcal{E}_{\max}$, in the inset of Fig. 1(a)]. Now the level spacing distribution $P(\Delta\mathcal{E})$ is obtained simply by generating a histogram for the spacings between all *successive* levels, $\Delta\mathcal{E}_i=\mathcal{E}_i-\mathcal{E}_{i-1}$, with sufficient number of bins.

In Fig. 1(a), we show a histogram for the distribution of level spacings corresponding to an oscillator with frequency ratio given by the golden mean, $R=\sigma_1\equiv(\sqrt{5}-1)/2$. To reveal the details, Fig. 1(a) is plotted on a log-log scale. The histogram is based on $N=10^6$ levels, and the number of bins is 10^5. One notices that, instead of a smooth convergent function as previously sought in $P(s)$ [4], $P(\Delta\mathcal{E})$ is sharply peaked only on a discrete set of values which decreases in an exponential fashion. Moreover, the height of these isolated peaks shows a highly regular increase in the form of an inverse-square law, as $\Delta\mathcal{E}$ is decreased.

To understand the level spacing distribution, we show in Fig.1(b) the level spacings, $\Delta\mathcal{E}_i=\mathcal{E}_i-\mathcal{E}_{i-1}$, plotted directly against the corresponding energy levels $\mathcal{E}_i$, again on a log-log scale. Note that this plot consists of individual points with each level $\mathcal{E}_i$ corresponding to a *unique* value $\Delta\mathcal{E}_i$. We see clearly that the level spacings are clustered on a discrete set of values that decrease exponentially as we go up in energy. The ''banded'' structure in Fig. 1(b) also suggests that certain values of the level spacings only correspond to a certain energy range. As a matter of fact, the x-axis (i.e., the energy levels) can be subdivided into consecutive sections with ''equal lengths'' (remember the log scale); in each of these sections $\Delta\mathcal{E}$ fluctuates only among three different values. When we enter the next section another value of $\Delta\mathcal{E}$ is born and it is lower than all three $\Delta\mathcal{E}$ values of the preceding section. At the same time the higher value of $\Delta\mathcal{E}$ from the previous section becomes inactive, therefore ensuring that there are only three active $\Delta\mathcal{E}$ values in the new section.

It turns out that the number theoretical properties of the frequency ratio R play a crucial role in understanding many details of our observation. For our chosen value of $R=\sigma_1$, the golden mean, we recall that σ_1 has a simple continued fraction expansion, $\sigma_1=[1,1,1,\ldots]$ [13], and its nth approximant is given by F_{n-1}/F_n. Here $\{F_n\}$ are the Fibonacci sequence defined by $F_0=0$, $F_1=1$, and $F_{n+1}=F_n+F_{n-1}$. It is easy to see from Eq. (3) that energy degeneracy is strictly forbidden for irrational R. Thus, as we increase $\mathcal{E}_{\max}$, the energy contour will never cross two lattice points simultaneously. However, it can cross two points in arbitrarily close succession. In particular, it crosses the point $\mathbf{m}=(F_{n-1},0)$ and $(0,F_n)$ in succession, and generates a level spacing $\Delta\mathcal{E}(F_n)=F_n|\sigma_1-F_{n-1}/F_n|$. Since F_{n-1}/F_n is closer to σ_1 than any other rational whose denominator does not exceed F_n [14,15], we conclude that $\Delta\mathcal{E}(F_n)$ is smaller than any $\Delta\mathcal{E}$ values that we encountered previously (i.e., with $\mathcal{E}_{\max}<F_{n-1}\approx F_n\sigma_1$). All the small level spacings are generated in this fashion during successive crossings of a pair of lattice points related to a pair of Fibonacci numbers. If one looks carefully in Fig.1(b), one will notice that the beginning of each horizontal row of points (except the first two rows) correspond to energy values that follow the Fibonacci sequence, $\mathcal{E}=1,2,3,5,8,13,21,\ldots$. Also, due to the property of the golden mean, $F_{n-1}-F_n\sigma_1=(-\sigma_1)^{n+1}$, all level spacings are integer powers of σ_1. Thus the entire distribution in this case satisfies

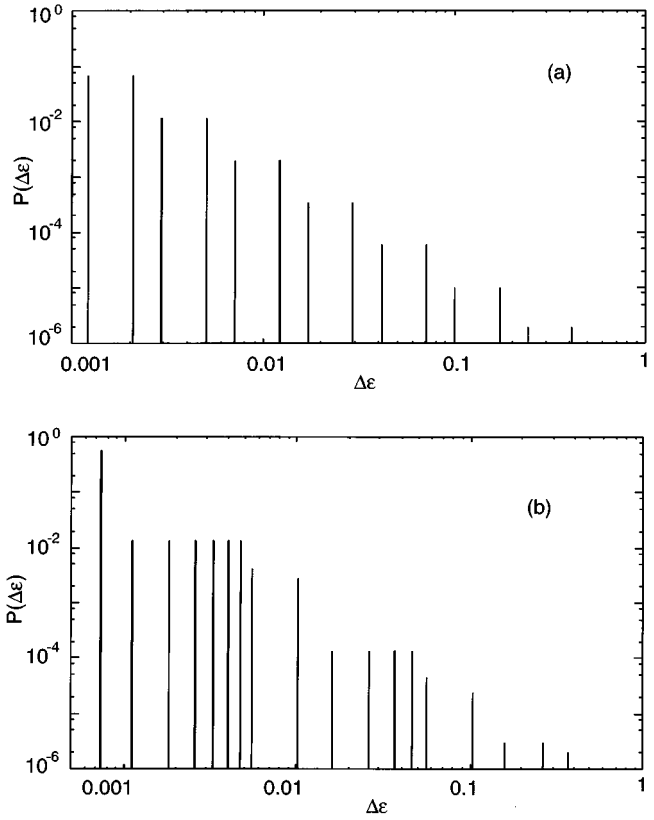

FIG. 2. Energy level spacing distribution for (a) $R=\sigma_2=\sqrt{2}-1$, and (b) $R=1/e$. These spectra are to be compared with the continued fraction expansions $\sigma_2=[2,2,\ldots]$ and $e=[1,2,1,1,4,1,1,6,\ldots]$.

$$P_{\sigma_1}(\Delta\mathcal{E})\propto\frac{1}{(\Delta\mathcal{E})^2}\,\delta(\Delta\mathcal{E}-\sigma_1^n),\quad n=1,2,3,\ldots. \tag{4}$$

From a physical point of view, the distribution in Fig. 1 demonstrates the importance of the classical periodic orbits in quasiperiodic systems, as in many other contexts regarding the classical-quantum correspondence [1]. For irrational R, the classical trajectory is always quasiperiodic and periodic (closed) orbits are strictly forbidden. However, any given section of a trajectory can be approximated very well by closed periodic orbits. For example, when $R=\sigma_1$, the trajectory is nearly periodic after F_{n-1} and F_n rotations along the two irreducible circuits, the difference is proportional to $|F_{n-1}-F_n\sigma_1|<1/F_{n+1}$ [14]. The longer the trajectory, the better the approximation (with accordingly longer period orbits). Therefore the *quantum* energy level spacing distribution in Fig. 1(a) can also be interpreted as a measure of the closeness of the *classical* quasiperiodic trajectory to the nearby periodic orbits, with the peak positions corresponding to the closeness in length, and the peak heights corresponding to the relative fraction of time the trajectory spends near the periodic orbits.

So far we have focused on a single value of the frequency ratio $R=\sigma_1$, mainly because of the number theoretical simplicity of the golden mean. Much of our observations, however, can be readily carried over to other irrational frequency ratios. In Fig. 2(a) we show the level spacing distribution for a slightly more complicated frequency ratio, $R=\sigma_2\equiv\sqrt{2}-1=[2,2,2,\ldots]$. Now $P(\Delta\mathcal{E})$ not only has peaks at $\Delta\mathcal{E}=|G_n\sigma_2-G_{n-1}|$, corresponding to the continued fraction approximations G_{n-1}/G_n (G_n can be found from, $G_0=0$, $G_1=1$ and $G_{n+1}=2G_n+G_{n-1}$), it also shows peaks that correspond to the so-called intermediate fractions $(G_n+G_{n-1})/(G_{n+1}+G_n)$ [15]. The intermediate fractions are in some sense the second best rational approximation to σ_2, since they would be the best approximations if we were to remove G_{n-1}/G_n from the real numbers. We see that the peak corresponding to the intermediate fraction $(G_n+G_{n-1})/(G_{n+1}+G_n)$ has the same height as the one corresponding to the continued fraction G_{n-1}/G_n, while the main peaks continue to follow the inverse-square law.

For general frequency ratio R, it is best approximated by the continued fractions $p_n/q_n=[a_1,a_2,\ldots,a_n]$. In addition, when $a_n>1$, there are a_n-1 intermediate fractions, $(p_{n-1}+kp_n)/(q_{n-1}+kq_n)$ $(k=1,2,\ldots,a_n-1)$, between p_{n-1}/q_{n-1} and p_n/q_n, which also provide a good approximation to R [15]. Pandey and co-workers [6,7] found a one-to-one correspondence between the allowed nearest neighbor level spacings of a 2DHO on one hand, and the continued and intermediate fraction approximations of the frequency ratio R on the other. In Fig. 2(b) we show a level spacing distribution for a transcendental number, $R=1/e$. We see that the peak positions agree with the predictions of Pandey and co-workers. In addition, we notice that the changes in the peak heights occur only for the main peaks corresponding to the continued fractions p_n/q_n (when $\mathcal{E}\approx p_n\approx q_nR$). All the a_n-1 intermediate peaks have the same height as the main peak that precedes them. In fact, in Fig. 2(b), if we start from the right and count groups of peaks with the same height, we obtain the sequence $e=[1,2,1,1,4,1,1,6,\cdots]$ [16]. This regular behavior of the peak heights seems to be true in general. In addition, if R belongs to a class of relatively simple irrationals known as quadratic numbers (which includes σ_1 and σ_2), the entire distribution is self-similar and shows a scaling behavior [17]. Indeed, if we replot the distribution of Figs. 1(a) and 2(a) using $(\Delta\mathcal{E})^2P(\Delta\mathcal{E})$ as the Y-axis, we obtain periodic spectra (on a log-log scale) with σ_1 and σ_2 as the periods (scaling factors) along the X axis. This is obviously related to the fact that the continued fraction expansion of a quadratic number is periodic [14]. The self-similarity in the level distribution is lost for a more general irrational R, but the overall inverse-square-law-type rise seems to persist, as seen in Fig. 2(b) for $R=1/e$.

Now we briefly discuss the level spacing distribution of the scaled spectrum, $P(s)$, with the scaled level spacing defined by $s_i\equiv N(\mathcal{E}_i)-N(\mathcal{E}_{i-1})$ [recall that $N(x)$ is the number of levels with $\mathcal{E}<x$]. This is the distribution originally considered by Berry and Tabor [4], and subsequently shown to be nonconvergent by Pandey and co-workers [6,7] For $R=1/\sqrt{2}$, by picking the same number of levels and bins, we were able to reproduce exactly the histogram in Fig. 5(a) of Ref. [4]. However, upon considering more levels and finer bins, the histogram shows oscillatory behavior and fails to converge. The conflict between the highly regular $P(\Delta\mathcal{E})$ (as in Figs. 1 and 2) and the nonconvergent $P(s)$ can be resolved, in our opinion, by noting an important fact: the average level spacing $\langle\Delta\mathcal{E}\rangle$ vanishes in the semiclassical limit. We can see this easily in the simple case of $R=\sigma_1$. According to Eq. (4),

$$\langle \Delta\mathcal{E} \rangle = \int_0^\infty P_{\sigma_1}(\Delta\mathcal{E}) \Delta\mathcal{E} d(\Delta\mathcal{E}) = \lim_{n\to\infty} \frac{\sum_{k=1}^{n} \frac{1}{\sigma_1^{2k}} \sigma_1^k}{\sum_{k=1}^{n} \frac{1}{\sigma_1^{2k}}}$$

$$= \lim_{n\to\infty} \frac{\sum_{k=1}^{n} \left(\frac{1}{\sigma_1}\right)^k}{\sum_{k=1}^{n} \left(\frac{1}{\sigma_1}\right)^{2k}} = 0. \tag{5}$$

We expect the above result to hold for arbitrary R in light of the inverse-square-law level spacing distribution favoring small $\Delta\mathcal{E}$. The purpose of using a scaled level spacing is to introduce a map $\mathcal{E}_i \to e_i$, such that the average spacing of the new levels, $s_i = e_i - e_{i-1}$, is unity (i.e., $\langle s \rangle = 1$). For a 2DHO, however, the original true level spacings have zero average and therefore it is impossible to find a map that can map it into a spectrum with unit average spacing. By formally defining, $e_i = N(\mathcal{E}_i)$, one ends up with a nonconvergent histogram. Another way to see this is to note that the system does not have a proper energy scale which one can use to normalize the level spacings. This is also reflected in the classical quasiperiodic trajectory, which does not have a unique time scale built in (such as the period of a closed periodic orbit).

Before closing, we would like to make some comment about the transition from the level spacing distribution of a 2DHO to that of the generic 2D integrable Hamiltonian system, namely, the Poisson distribution. First we recall that what makes a harmonic oscillator different from generic integrable systems is its flat energy contour in action space [4]. This makes a harmonic oscillator with incommensurate frequency ratios a ''permanently'' quasiperiodic system, in the sense that the frequency ratio R is energy independent. Once R is given, the classical trajectory remains topologically the same regardless of the energy. Thus the corresponding quantum energy levels only reflect the particular value of R. This is not the case for generic integrable systems, where the frequencies $\omega_i(\mathbf{I}) = \partial\mathcal{H}(\mathbf{I})/\partial I_i = \omega_i(\mathbf{I} = \mathbf{m}\hbar)$ depend on the values of the actions, which in turn is determined by energy. As we increase the energy range $\mathcal{E}_{\max}$, R varies smoothly and the ''memory'' for a particular frequency ratio is lost in the overall quantum level spectrum, so is the the correlation between different levels. As a result, the level spacing is essentially random, and we have a Poisson-like distribution. It seems reasonable then that the generic Poisson distribution might arise as a result of an effective averaging of the harmonic oscillator level spectrum over all possible frequency ratios. Further studies are needed, however, to establish such a connection. Finally we note that the two-dimensional harmonic oscillator is not only interesting on its own right, it also serves as a good model system for small quantum dots in semiconductor heterostructures [18,19].

The author would like to thank Terry Orlando for helpful discussions. Financial support for this project is provided by the National Science Foundation under Grant No. DMR-9402020 and the U.S. Air Force Office of Scientific Research under Grant No. F49620-95-1-0311.

[1] Martin C. Gutzwiller, *Chaos in Classical and Quantum Mechanics* (Springer, New York, 1990).
[2] Edward Ott, *Chaos in Dynamical Systems* (Cambridge University Press, Cambridge, 1993).
[3] M. Tabor, *Chaos and Integrability in Nonlinear Dynamics* (Wiley-Interscience, New York, 1989).
[4] M. V. Berry and M. Tabor, Proc. R. Soc. London, Ser. A **356**, 375 (1977).
[5] O. Bohigas, M. J. Giannoni, and C. Schmit, Phys. Rev. Lett. **5**, 1 (1984).
[6] A. Pandey, O. Bohigas, and M. J. Giannoni, J. Phys. A **22**, 4083 (1989).
[7] A. Pandey, and R. Ramaswamy, Phys. Rev. A **43**, 4237 (1991).
[8] P. M. Bleher, J. Stat. Phys. **61**, 869 (1990); **63**, 261 (1991).
[9] C. D. Greenman, J. Phys. A **29**, 4065 (1996).
[10] M. Kohmoto, L. P. Kadanoff, and C. Tang, Phys. Rev. Lett. **50**, 1870 (1983).
[11] S. Ostlund, R. Pandit, D. Rand, H. J. Schellnhuber, and E. D. Siggia, Phys. Rev. Lett. **50**, 1873 (1983).
[12] T. Geisel, R. Ketzmerick, and G. Petschel, Phys. Rev. Lett. **66**, 1651 (1991).
[13] Here we adopt the notation of a continued fraction,

$$[a_1, a_2, a_3, \ldots] \equiv \cfrac{1}{a_1 + \cfrac{1}{a_2 + \cfrac{1}{a_3 + \cdots}}}.$$

[14] G. H. Hardy and E. M. Wright, *An Introduction to the Theory of Numbers*, 4th ed. (Clarendon, Oxford, 1960).
[15] A. Ya. Khinchin, *Continued Fractions* (University of Chicago Press, Chicago, 1964).
[16] Without loss of generality, we consider $R < 1$ in this paper, since R and $1/R$ are number theoretically equivalent (see Ref. [14]).
[17] S. J. Shenker and L. P. Kadanoff, J. Stat. Phys. **27**, 631 (1982).
[18] A. Kumar, S. E. Laux, and F. Stern, Appl. Phys. Lett. **54**, 1270 (1989).
[19] C. B. Whan and T. P. Orlando (unpublished).